

# Partial photoionization cross sections of C<sub>60</sub> and C<sub>70</sub>: A gas versus adsorbed phase comparison

S. Korica<sup>a</sup>, A. Reinköster<sup>a</sup>, M. Braune<sup>a</sup>, J. Viehhaus<sup>a,\*</sup>, D. Rolles<sup>a,†</sup>, B. Langer<sup>b</sup>, G. Fronzoni<sup>c</sup>, D. Toffoli<sup>c</sup>, M. Stener<sup>c</sup>, P. Decleva<sup>c</sup>, O. M. Al-Dossary<sup>d</sup>, U. Becker<sup>a,d</sup>

<sup>a</sup>Fritz-Haber-Institut der Max-Planck-Gesellschaft, Faradayweg 4-6, D-14195 Berlin, Germany

<sup>b</sup>Physikalische und Theoretische Chemie, Freie Universität Berlin, Takustraße 3, D-14195 Berlin, Germany

<sup>c</sup>Dipartimento di Scienze Chimiche, Università di Trieste, Via L. Giorgieri 1, I-34127 Trieste, Italy

<sup>d</sup>Physics Department, College of Science, King Saud University, Riyadh, 11451, Saudi Arabia

## ARTICLE INFO

### Keywords:

Synchrotron radiation photoelectron spectroscopy  
Photoelectron emission  
Fullerenes  
Density functional calculations

## ABSTRACT

We have performed high resolution measurements of the photoelectrons emitted from the valence shell of C<sub>70</sub>, in the gas and adsorbed phase on a metal surface, in order to derive branching ratios and the partial photoionization cross sections of the two highest occupied molecular orbitals, HOMO and HOMO-1. The comparison between the two phases and the adsorbed phase shows an interesting and unexpected difference that can be attributed to a small orbital shift in solid C<sub>70</sub>. Density Functional Theory calculations within the Local Density Approximation (LDA) show good agreement for both data sets and give a plausible explanation for the observed difference.

## 1. Introduction

The discovery of the family of carbon molecules dubbed the 'fullerenes' [1] and the breakthrough in their synthesis [2] have stimulated an extensive research activity in this field. The best known among the fullerenes is the C<sub>60</sub> molecule, which consists of 60 carbon atoms arranged on a nearly spherical shell with the highest possible symmetry, point group I<sub>h</sub>. Recently, we have studied some of its particularly interesting properties by photoelectron spectroscopy [3]. Our results revealed strong oscillations in the partial photoionization cross sections of the two highest occupied molecular orbitals, HOMO and HOMO-1, reflecting the molecular geometry and symmetry of the electronic charge distribution.

These oscillations, which were for the first time discovered in solid C<sub>60</sub> and interpreted as a solid state effect [4,5], were later also observed for free C<sub>60</sub> molecules [6]. Their interpretation was basically interpreted within a standing wave model of the photoelectron wave in a box like potential [7] being extended to a jellium like potential in a subsequent experimental and theoretical study [8]. It is the spherical like structure of the C<sub>60</sub> molecule which gives rise to shell like distribution of the delocalized carbon valence electrons. However, one may look to the problem also from the view point of symmetry. The valence hole states HOMO and HOMO-1 have different symmetry *gerade* (*g*) and

*ungerade* (*u*), a situation which may be compared to homonuclear diatomic molecules. Here the *g* and *u* states show also pronounced oscillations in their partial photoionization cross sections and even more pronounced oscillations in their photoelectron diffraction intensity behavior in the molecular frame. These oscillations which were predicted more than forty years ago by Cohen and Fano [9] have been experimentally corroborated since the last ten years only [10,11]. Regarding photoionization this was even more recently [12]. The showcase example exhib-

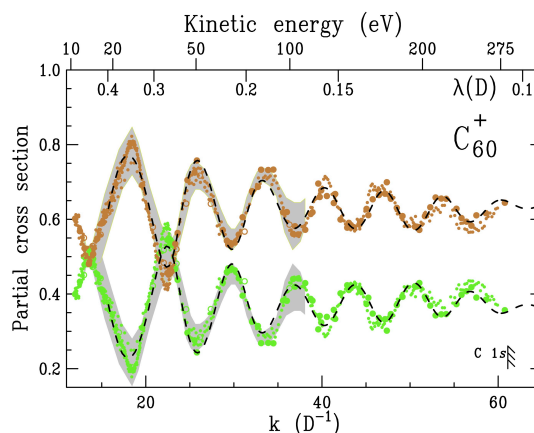


**Fig. 1** The normalized partial cross section of the HOMO and HOMO-1 orbitals of C<sub>60</sub> derived from partial and branching ratio measurements. The data points from the ref. [3] are given by small filled circles, from the ref. [8] by bigger filled circles whereas from the ref. [6] are given by open circles.

Corresponding Author. Tel.: +49 30 8413 5694; fax +49 30 8413 5695

E-mail address: becker\_u@fhi-berlin.mpg.de (Uwe Becker)

\*Present address: DESY, Notkestraße 85, D-22603 Hamburg, Germany

†Present address: Max Planck Advanced Study Group, Center for Free Electron Laser Science (CFEL), D-22761 Hamburg, Germany

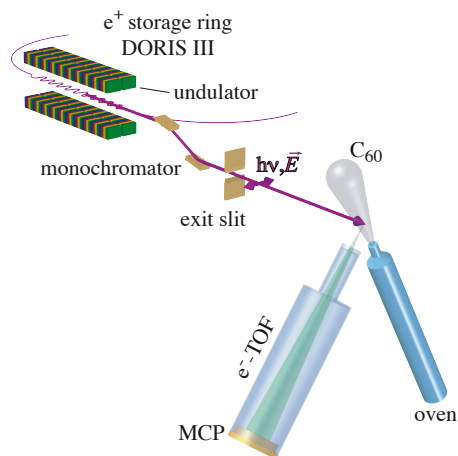


**Fig. 2** Scheme of the experimental set-up for the photoelectron spectroscopy experiment using a time-of-flight (TOF) analyzer and a molecular beam source at HASYLAB.

iting oscillations over several periods is the core electron photoionization of  $N_2$  [13]. The oscillation frequency is proportional to the bond length  $R$  in the same respect as the oscillation frequency is proportional to the diameter  $D$  of  $C_{60}$ . In this sense these two may be directly compared if one chooses for the kinetic energy axis the reciprocal bond length or the diameter as unit of the electron momentum. In Fig. 1 we show the normalized partial cross section of the HOMO and HOMO-1 orbitals of  $C_{60}$  derived from partial cross section and branching ratio measurements during the last years [3]. The normalization was done with respect to the non-oscillating intensity in order to remove this steeply declining part and to exhibit the oscillation over a large energy range more clearly. The dashed curve represents the corresponding part of the fitting curve. The oscillations cover de Broglie wavelengths of the photoelectron down to  $\lambda(D) = 0.1$  corresponding to ten full oscillation periods in the carbon cage. These properties of  $C_{60}$  are very similar in both the gas and solid phase due to the weak van der Waals forces that bind the solid. We have now performed the same kind of experiments as for  $C_{60}$  also for  $C_{70}$ , the next most stable molecule of the fullerene family, in the gas phase and also in a noncrystalline adsorbed formation. Our results show an unexpected different behavior. The oscillations of the HOMO/HOMO-1 branching ratio exhibit a

distinct offset between the gas and solid phase curves pointing to a relative orbital shift upon absorption.

## 2. Experiment

Our measurements were carried out at the undulator beam-line BW3 of the Hamburger Synchrotron Radiation Laboratory HASYLAB at DESY [14]. Synchrotron radiation was monochromatized in a modified SX-700 plane grating monochromator with a usable energy range of approximately 20-2000 eV and a spectral resolution of 0.1 eV in the energy range applied here. The experimental set-up is presented at Fig. 2. An effusive molecular beam was produced by a resistively heated oven at 500°C which contained 98%-purified  $C_{70}$  powder. For the solid state measurements the  $C_{70}$  fullerenes were deposited on an OFHC-copper substrate kept at room temperature and positioned at the angle of 45° with respect to the direction of the incoming light. The angle between the surface normal and photoelectron emission and the angle between the surface normal and the polarization plane were 19° and 51°, respectively. After the ionization of the target with the synchrotron light the outgoing electrons were detected in a time-of-flight (TOF) electron spectrometer, placed at the magic angle (54.7°) which monitors the partial cross section independently from the angular distribution. Appropriate voltages can be applied to the spectrometer in order

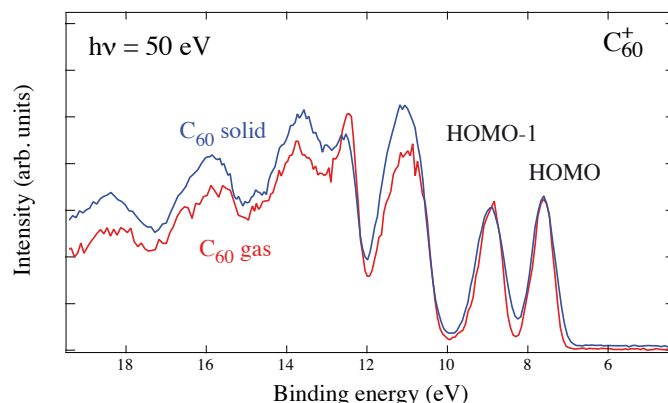


**Fig. 4** Photoelectron spectra for the solid and gas phase  $C_{60}$  taken at the photon energy of 50 eV.

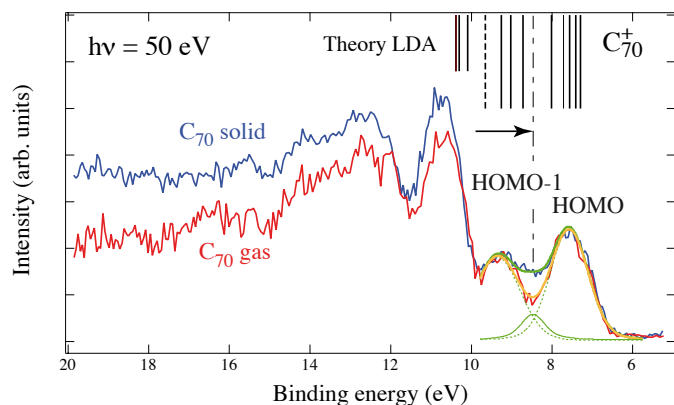


**Fig. 3** Photoelectron spectra for the solid and gas phase  $C_{70}$  taken at the photon energy of 50 eV. The results are compared with the theoretical calculations within the frame of LDA given by the vertical bars. The dashed-dotted line depicts the position of the filled HOMO HOMO-1 gap. The green solid and dashed lines represent the fitted curves to the additional intensity observed in the adsorbed phase.

to keep a constant resolution of the electron spectra for different photon energies. More details of the experimental apparatus are given in reference [3]. The spectra were recorded in the photon energy range from 25 eV to 200 eV with the steps of 1 eV for the solid and with the steps of 5 eV for the gas phase.

## 3. Results and discussion

A typical photoelectron spectrum for both, solid and the gas phase, at incident photon energy of 50 eV is presented at Fig. 3. The vertical bars represent the result of the Density Functional Theory (DFT) calculations within the Local Density Approximation (LDA) shifted so that the calculated first ionization energy aligns with the measured first vertical ionization energy. Note that our experimentally obtained first ionization potential of approximately 7.6 eV is in good agreement with *ab initio* Hartree-Fock calculations [15] and is 0.27 eV lower than for  $C_{60}$  obtained at the same level of theory [16]. In the LDA calculations of Density Functional Theory explored here, all many-body effects are collected into the exchange-correlation energy, evaluated within a free-electron model. The computational ap-

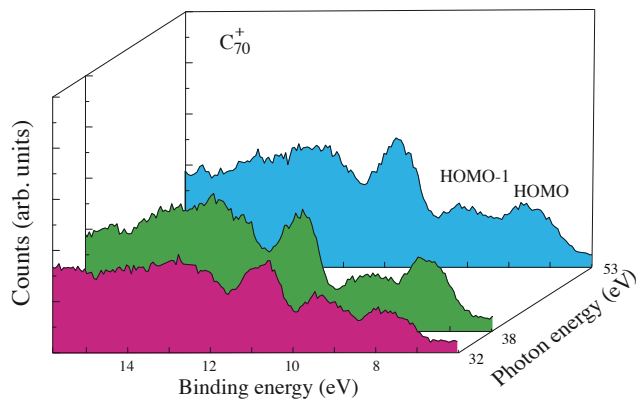


**Fig. 5** Photoelectron yield, for the solid  $C_{70}$ , measured at the magic angle ( $54.7^\circ$ ), which is proportioned to the partial cross section, as a function of the binding energy for three different photon energies.

proach employed accurately solves the Kohn-Sham equations, both in the discrete and continuous spectrum, using a multi-center basis of B-spline functions. Bound state orbitals are obtained by conventional diagonalization, while the full set of open channel continuum orbitals are obtained by a least squares approach. The initial ground state density is obtained using a conventional LCAO calculation, employing the Amsterdam density functional program and a double zeta plus polarization basis. This affords a numerically convergent solution of the Schrödinger equation in a realistic one-particle potential, and gives a good reproduction of the available experimental data. More details of the procedure are given elsewhere [17,18]. Our experimental results are also in good agreement with some other theo-

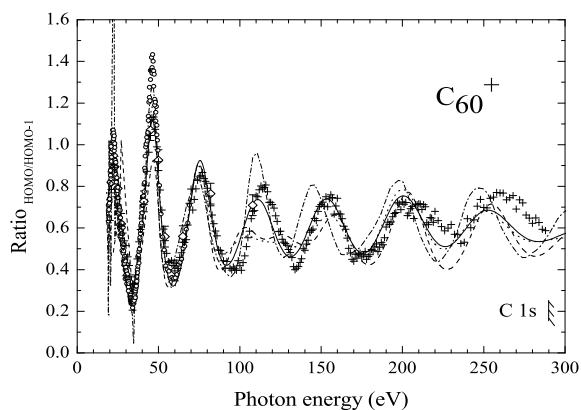


**Fig. 6** Partial cross-section ratio HOMO/HOMO-1 for gas and solid  $C_{60}$  for different photon energies. The lines show the results of different theoretical models: theoretical curves with a Jellium model (-----) and with LDA calculations (-----); semi-empirical curves with a Shell model (.....) and with a Shell+Cage model (—). The experimental data of ref. [8] are shown by open rhombs, whereas the data of our previous work [3] are given by open circles for the gas phase data and crosses for the solid state measurements.

retical calculations [15,19,20], the latter one also employing LDA to calculate electronic structure by using molecular orbitals constructed from linear combination of Gaussian-type functions. Both, theory and experiment, reveal sharp and well defined structures in the low binding energy region of the spectrum which points to the high degeneracy of the electronic levels as expected from the relatively high symmetry of the molecule and in general to the weak interaction between the fullerene molecules. The states closest to the Fermi level  $E_F$ , for the solid  $C_{70}$

are derived from the molecular HOMO which is of  $a_2''$  symmetry, and some deeper-lying  $\pi^*$  molecular orbitals HOMO-1 of  $e_2''$  symmetry [21]. HOMO and HOMO-1 are representing 20 electrons in largely  $\pi$ -derived levels. Other photoelectron lines are very broad and not well resolved. The comparison with our present and previous gas phase measurements of  $C_{70}$  [22-24] reveals close similarity indicating that the molecules in the molecular crystal, bounded by weak van der Waals forces, behave in many respects like free molecules. However, the relative intensities of the valence photoemission lines of solid and gaseous  $C_{70}$  are different, probably because of inelastic scattering effects and differences in the corresponding transition matrix elements. In order to quantify this effect, we have made a fit to the associated structures shown in figure 3. The comparison of the  $C_{70}$  with the  $C_{60}$  spectra (Fig. 4 and Ref. [3]) reveals also close similarity. The molecular elongation of  $C_{60}$  because of the 10 additional carbon atoms around the equator in order to produce  $C_{70}$  has little effect on the overall distribution of bands. That means however that for  $C_{70}$  there will be five additional  $p_\pi$ -derived bands in the vicinity of HOMO. Moreover the spectra do differ because the breaking of the  $I_h$  symmetry in  $C_{60}$  into  $D_{5h}$  in  $C_{70}$  leads to lowering of the degeneracies of the energy levels and broadening and splitting of the photoelectron lines. In  $C_{60}$ , HOMO and HOMO-1 have no discernible underlying structure whereas in  $C_{70}$ , the corresponding features split into three resolvable photoelectron features in the first peak and two in the second [19].

Fig. 5 shows photoelectron spectra for three different photon energies for the solid state  $C_{70}$ . Our results show oscillations in the intensity, or in other words, in the partial cross section of the two outermost molecular orbitals, HOMO and HOMO-1 as a function of the photon energy. These oscillations are well known for the case of  $C_{60}$  [3,4,6,8] for both gas and the solid phase but, due to the reduced symmetry, less pronounced for the case of  $C_{70}$ . For the same reason, they exhibit much quicker damping at higher photon energies. The crucial point for understanding of this phenomenon is the importance of the spherical structure of fullerene molecules. According to the spherical shell model [7], the variations of the photoionization cross sections are due to the formation of the spherical standing waves of the final state elec-

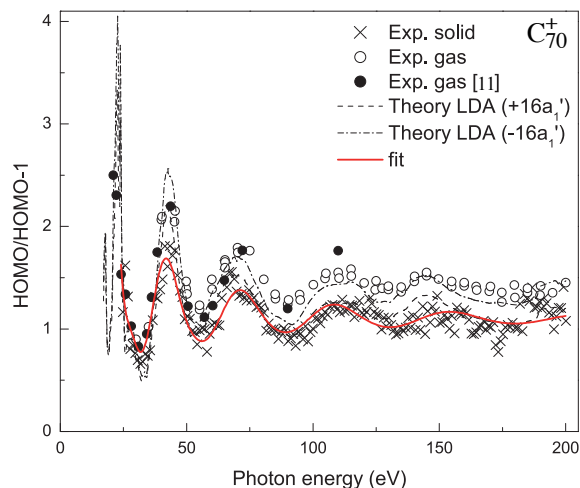


**Fig. 7** Partial cross section ratio HOMO/HOMO-1 for gas and solid  $C_{70}$  for different photon energies. The experimental data of the present work are shown by open circles and of ref. [23] by filled circles for the gas phase, whereas the data of the present work for the solid state measurements are given by crosses. The dashed lines show the calculated results based on the LDA with (-----) and without (.....) the  $16a_1'$  orbital. The solid curve is the result of our semi-empirical fit.

trons inside the molecule. This effect may be considered as intramolecular interference. Higher fullerenes, e.g.  $C_{84}$  [25],  $C_{78}$ ,  $C_{82}$ ,  $C_{86}$ ,  $C_{90}$  and  $C_{96}$  [26-28] showed similar photoemission intensity variations in the solid state. These results first pointed to a fullerene-specific phenomenon but just recently, it has been shown that it is a much more widespread behavior, even present in transition metal sandwich molecules [29].

The branching ratio of the HOMO and HOMO-1 photolines for  $C_{70}$  is shown in Fig. 7. For the comparison, the result of our previous work with  $C_{60}$  is given in Fig. 6. Using this ratio one avoids uncertainties produced by photon beam intensity fluctuations. The solid line is the result of the semi-empirical model where the data are approximated by an exponentially decaying set of spherical Bessel functions, including electronic and geometric properties of  $C_{70}$ . Using a Levenberg-Marquardt algorithm for an estimation of the fitted parameters we have obtained values close to the measured ones. Considering the experimental results, the ratio between the corresponding HOMO and HOMO-1 levels shows an offset of about 0.5 for the gas phase measurements compared to solid state data. The latter one are constantly lower for all energies between 25 and 200 eV. As already pointed out, the molecular elongation of  $C_{60}$  in order to produce  $C_{70}$  introduces 10 additional carbon atoms around the equator of the molecule. According to the calculations of Mintmire and co-workers [20], this results in an increase of s-derived to p-derived emission lines for  $C_{70}$  with increasing photon energy. Moreover, the elongation of the  $C_{70}$  cage probably introduces orientational disorder in the solid. According to our calculations, the HOMO band comprises 6 ionizations, for a total of 20 electrons, compared to the 10 electrons in the corresponding

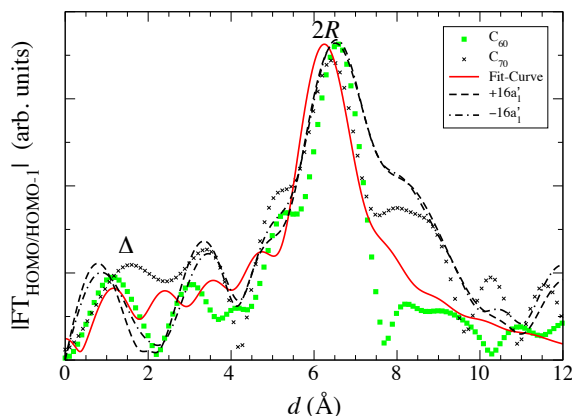


**Fig. 8** Fourier-transform magnitude of the cross section ratios for the solid  $C_{70}$ . Experimental results are given by crosses and the result of the model fitted function taken from Fig. 7 is given by the solid line. For the comparison, the Fourier-transform of the two theoretical curves, with and without additional orbital, is also presented. The result of solid  $C_{60}$  taken from the ref. [3] is given by the solid squares.

ungerade band of  $C_{60}$ , and the next band, HOMO-1, is formed by 4 or 5 different ionizations, for a total of 16 to 18 electrons. Theoretical calculations show good agreement for our both data sets, if one assumes, that in the gas phase the  $16a_1'$  orbital (Fig. 3, dashed line) which lies at the bottom of the HOMO-1 band is part of the next peak. We assume, that upon adsorption this band becomes filled but with a relative orbital shift from the tail of HOMO-2 (gas phase) towards the HOMO-1 band thereby moving the latter one closer to the HOMO band and filling the gap partially. This, however, has to be independently corroborated and further explored by future studies.

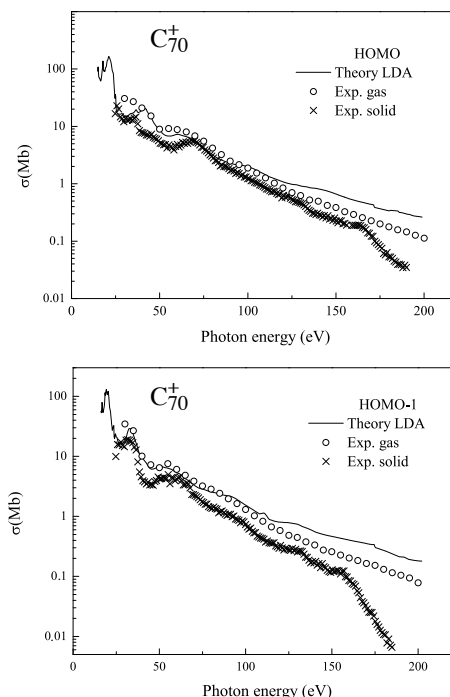


**Fig. 9** Absolute cross section for the two outermost orbitals of  $C_{70}$ , HOMO (upper part) and HOMO-1 (lower part). The experimental points are given by open circles for the gas phase data and by crosses for the solid state data. We show the full range of the partial cross section behavior for comparison with Fig. 7, but assume that the sudden drop of the partial cross sections at the end of the photon energy range comes rather from the variations of the beamline's flux than the molecule itself. The solid line represents our theoretical curve based on the LDA.

The Fourier transformation of the HOMO/HOMO-1 ratio (Fig. 8) enables us to extract the structural information about the molecule like the cage radius ( $R$ ) and the thickness of the electron cloud ( $\Delta$ ). The radius of the molecule obtained in this way is in good agreement with what one would expect after averaging over all the axis of this ellipsoidally shaped fullerene [30]. The transformed experimental data show more structures at larger distances than the simple model and the shape of the  $C_{70}$  experimental curve is broader than in the case of  $C_{60}$  because of its lower symmetry.

Fig. 9 shows the partial cross section of the  $C_{70}$ 's two outermost orbitals. The overall agreement between theory and experiment is good. The photoionization cross sections exhibit an oscillatory behavior with a frequency related to the diameter of the fullerene molecule superimposed on the exponential decay. Previous measurements [22,23] were not performed at sufficiently close energy intervals to prove the more detailed structure of these oscillations. They can be explained by single-particle effects [31], i.e. the collective response of the valence electron cloud to the electromagnetic radiation appears to play a negligible role in this respect.

#### 4. Conclusion

In summary, for the first time we, have performed the systematic measurements of the photoelectron spectra of  $C_{70}$ , for both, the gas and the adsorbed phase, in small energy steps over a wide energy range. We have shown that the partial cross section oscillations in the fullerenes  $C_{60}$  and  $C_{70}$  are not only a sensitive measure of their particular electronic and geometric structure but also of their environment. This is demonstrated for the case of  $C_{70}$  where this ratio, in contrast to the case of  $C_{60}$ , shows a marked difference depending on the molecular environment

either in the gas or adsorbed phase. This change in behavior is suggested to be caused by a small orbital shift in C<sub>70</sub>.

## References

- [1] H. W. Kroto, J. R. Heath, S. C. O'Brien, R. F. Curl, and R. E. Smalley, *Nature* 318 (1985) 162.
- [2] W. Krätschmer, L. D. Lamb, K. Fostiropoulos, and D. R. Huffman, *Nature* 347 (1990) 354.
- [3] S. Korica, D. Rolles, A. Reinköster, B. Langer, J. Viehhaus, S. Cvejanović, and U. Becker, *Phys. Rev. A* 71 (2005) 13203.
- [4] P. J. Benning, D. M. Poirier, N. Troullier, J. L. Martins, J. H. Weaver, R. E. Haufler, L. P. F. Chibante, and R. E. Smalley, *Phys. Rev. B* 44 (1991) 1962.
- [5] J. Wu, Z. Shen, D. Dessau, R. Cao, D. Marshall, P. Pianetta, I. Lindau, X. Yang, J. Terry, D. King, B. Wells, D. Elloway, H. Wendt, C. Brown, H. Hunziker, and M. de Vries, *Physica C* 197 (1992) 251.
- [6] T. Liebsch, O. Plotzke, F. Heiser, U. Hergenbahn, O. Hemmers, R. Wehlitz, J. Viehhaus, B. Langer, S. B. Whitfield, and U. Becker, *Phys. Rev. A* 52 (1995) 457.
- [7] Y. B. Xu, M. Q. Tan, and U. Becker, *Phys. Rev. Lett.* 76 (1996) 3538.
- [8] A. Rüdel, R. Hentges, U. Becker, H. S. Chakraborty, M. E. Madjet, and J. M. Rost, *Phys. Rev. Lett.* 89 (2002) 125503.
- [9] H. D. Cohen and U. Fano, *Phys. Rev.* 150 (1966) 30.
- [10] N. Stollerfoht, B. Sulik, V. Hoffmann, B. Skogvall, J. Y. Chesnel, J. Rangama, F. Frémont, D. Hennecart, A. Cassimi, X. Husson, A. L. Landers, J. A. Tanis, M. E. Galassi, and R. D. Rivaola, *Phys. Rev. Lett.* 87 (2001) 23201.
- [11] D. Misra, U. Kadhane, Y. P. Singh, L. C. Tribedi, P. D. Fainstein, and P. Richard, *Phys. Rev. Lett.* 92 (2004) 153201.
- [12] X. -J. Liu, N. A. Cherepkov, S. K. Semenov, V. Kimberg, F. Gel'mukhanov, G. Prümper, T. Lischke, T. Tanaka, M. Hoshino, H. Tanaka, and K. Ueda, *J. Phys. B* 39 (2006) 4801.
- [13] B. Zimmermann, D. Rolles, B. Langer, R. Hentges, M. Braune, S. Cvejanović, O. Gefner, F. Heiser, S. Korica, T. Lischke, A. Reinköster, J. Viehhaus, R. Dörner, V. McKoy, and U. Becker, *Nature Physics* 4 (2008) 649.
- [14] S. Larsson, A. Beutler, O. Björneholm, F. Federmann, U. Hahn, A. Rieck, S. Verbin, and T. Möller, *Nucl. Instrum. Methods. Phys. Res. A* 337 (1994) 603.
- [15] G. Scuseria, *Chem. Phys. Lett.* 180 (1991) 451.
- [16] G. Scuseria, *Chem. Phys. Lett.* 176 (1991) 423.
- [17] M. Venuti, M. Stener, G. De Alti, and P. Decleva, *J. Chem. Phys.* 111 (1999) 4589.
- [18] M. Stener, S. Furlan, and P. Decleva, *J. Phys. B* 33 (2000) 1081.
- [19] D. L. Lichtenberg, M. E. Rempe, and S. B. Gogosha, *Chem. Phys. Lett.* 198 (1992) 454.
- [20] J. W. Mintmire, B. I. Dunlap, D. W. Brenner, R. C. Mowrey, and C. T. White, *Phys. Rev. B* 43 (1991) 14281.
- [21] D. R. Lawson, D. L. Feldheim, C. A. Foss, P. K. Dorhout, C. M. Elliott, C. R. Martin, and B. Parkinson, *J. Phys. Chem.* 96 (1992) 7175.
- [22] B. Langer, A. Wills, G. Prümper, R. Hentges, and U. Becker, *HASYLAB Annual Report*, 215 (2000).
- [23] T. Liebsch, O. Plotzke, R. Hentges, A. Hempelmann, U. Hergenbahn, F. Heiser, J. Viehhaus, U. Becker, and Y. Xu, *J. Electr. Spectrosc. Relat. Phenom.* 79 (1996) 419.
- [24] T. Liebsch, R. Hentges, A. Rüdel, J. Viehhaus, U. Becker, and R. Schlögel, *Chem. Phys. Lett.* 279 (1997) 197.
- [25] S. Hino, K. Matsumoto, S. Hasegawa, K. Kamiya, H. Inokuchi, T. Morikawa, T. Takahashi, K. Seki, K. Kikuchi, S. Suzuki, I. Ikemoto, and Y. Achiba, *Chem. Phys. Lett.* 190 (1992) 169.
- [26] S. Hino, K. Matsumoto, S. Hasegawa, K. Iwasaki, K. Yakushi, T. Morikawa, T. Takahashi, K. Seki, K. Kikuchi, S. Suzuki, I. Ikemoto, and Y. Achiba, *Phys. Rev. B* 48 (1993) 8418.
- [27] S. Hino, T. Takahashi, K. Iwasaki, T. Miyazaki, K. Kikuchi, and Y. Achiba, *Chem. Phys. Lett.* 230 (1994) 165.
- [28] S. Hino, K. Umishita, K. Iwasaki, T. Miyazaki, K. Kikuchi, and Y. Achiba, *Phys. Rev. B* 53 (1996) 7496.
- [29] P. Decleva, G. Fronzoni, M. Stener, M. de Simone, M. Coreno, J. C. Green, N. Hazari, and O. Plekan, *Phys. Rev. Lett.* 95 (2005) 263401.
- [30] W. Andreoni, F. Gugi, and M. Parrinello, *Chem. Phys. Lett.* 189 (1992) 241.
- [31] O. Frank and J. M. Rost, *Phys. Rev. A* 60 392 (1999) 392.